Supporting Information

Tough Coating Proteins: Subtle Sequence Variation Modulates Cohesion

Saurabh Das[a], Dusty R. Miller[b], Yair Kaufman[a], Nadine R. Martinez Rodriguez[c], Alessia Pallaoro[d], Matthew J. Harrington[f], Maryte Gylys[d], Jacob N. Israelachvili[a, e, 1], J. Herbert Waite[b, c, d, e, 1]

[a]Department of Chemical Engineering, University of California, Santa Barbara, California 93106, USA, [b]Biomolecular Science and Engineering, University of California, Santa Barbara, California 93106, USA; [c]Department of Molecular, Cell & Developmental Biology, University of California, Santa Barbara, California 93106, USA; [d]Department of Chemistry and Biochemistry, University of California, Santa Barbara, California 93106, USA; [e]Materials Research Laboratory, University of California, Santa Barbara, California 93106, USA. [f]Department of Biomaterials, Max Planck Institute for Colloids and Interfaces, 14424 Potsdam-Golm, Germany.

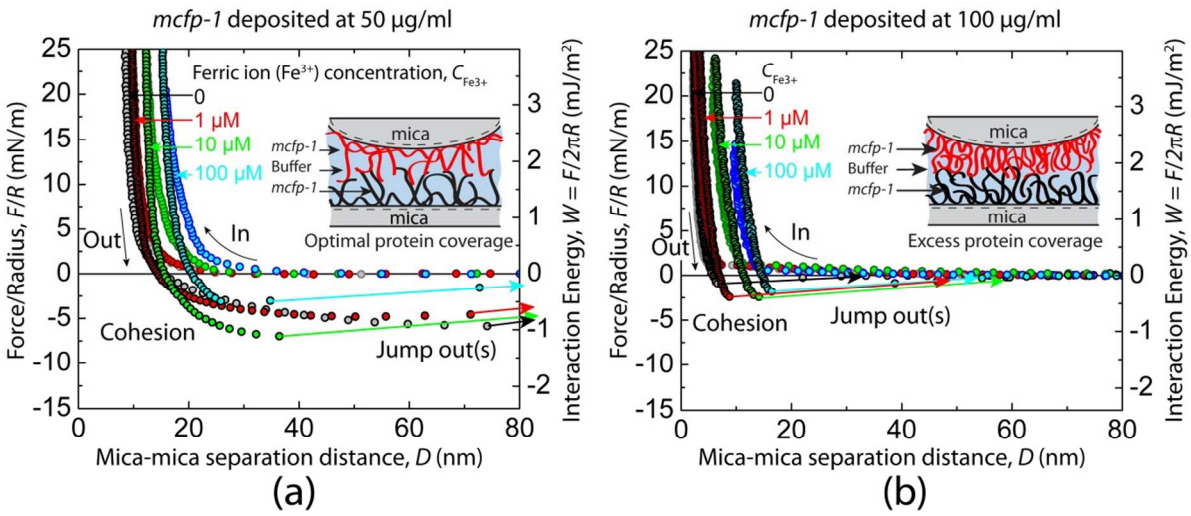

Figure S1. Representative force *vs.* distance plot showing cohesion between two symmetric *mfp-1*(*Mc*) films deposited at (a) C_{fp1} = 50 µg/ml and (b) 100 µg/ml in 0.1 M sodium acetate buffer, pH 5.5, 0.25 M KNO_3, and 1 mM bis-tris with C_{Fe3+} = 0 µM (gray), C_{Fe3+} = 1µM (red), 10 µM (green) and 100 µM (blue). In all cases the surfaces were brought into short contact (1-2 min).

Cohesive interactions between *mfp-1* (*Mc*) films. At low protein deposition concentrations ($C_{fp1} \leq 10$ µg/ml), *mfp-1* (*Mc*) forms a patchy film (Fig. 4a and a') on the mica surface with all or most of the Dopa and Lys ε-amino ($-NH_3^+$) groups bound to the mica crystal lattice and robustly binding the mfp-1 film to mica. Hence, few of the Dopa and Lys side-chains in the *mfp-1* (*Mc*) film on one of the mica surfaces are available for adhering the protein to the opposing surface, resulting in low or no adhesion/cohesion between the surfaces for $C_{fp1} \leq 10$ µg/ml. At the optimal protein deposition concentration (C_{fp1} = 50 µg/ml) for cohesion, some of the Dopa and Lys residues help to bind the protein film to the mica surface whereas the others not bound to mica are available to adhere the film to the opposing mica surface (asymmetric) or the protein film (symmetric) on the other surface.

The energy of adhesion between the *mfp-1* (*Mc*) film and the opposing mica surface initially increases (Fig. S3, S4) from C_{fp1} = 10 to 50 μg/ml, then levels off for C_{fp1} > 50 μg/ml presumably because the number of exposed Dopa and Lys side-chains responsible for the adhesion of the protein film to the mica surface increases with increase in C_{fp1} and does not change for higher protein film deposition concentrations (C_{fp1} > 50 μg/ml). Refractive index (n_F) measurements (Table S2) of the confined protein film showed that at high protein deposition concentrations (C_{fp1} > 50 μg/ml), the surface gets crowded with the protein molecules. Thus, the volume fraction of *mfp-1* (*Mc*) in the hydrated protein film increased progressively from 9 to 71 % as C_{fp1} was increased from 10 to 100 μg/ml, implying that at higher protein film deposition concentrations, the density of *mfp-1* (*Mc*) in the film increases.

Hence, for two interacting protein films (symmetric), a smaller cohesive force was measured between the surfaces although the number of Dopa and Lys groups interacting across interface stays constant due to the steric repulsion induced by the *mfp-1* (*Mc*) molecules crowding the mica surfaces (Fig 2). Hence for the cohesion measurements, W_c reaches a maximum value as C_{fp1} is increased.

Adhesive interactions of *mfp-1* (*Mc*) film to mica. A surfaces forces apparatus (SFA) was used to investigate the adhesive interactions of *mfp-1* (*Mc*) to a mica surface (i.e., asymmetric configuration, see Fig. S3a and S4) at various protein deposition concentrations (C_{fp1} = 10, 25, 50 and 100 μg/ml). The forces measured on approach of the surfaces were purely repulsive for protein deposition at C_{fp1} = 10-100 μg/ml (Fig. S3a and S4). Negligible adhesion was measured between the *mfp-1* (*Mc*) film and the mica surface during separation for C_{fp1} = 10 μg/ml (Fig. S3b and S4).

Increasing the protein film deposition concentration C_{fp1} to 25 μg/ml resulted in a "jump out" when separating the surfaces (Fig. S3a) indicating adhesive contact between the *mfp-1* (*Mc*) film and the mica surface with an adhesion energy, W_{ad} = 0.79 ± 0.25 mJ/m^2 (Fig. S3b). For C_{fp1} = 50 μg/ml, the protein film adhered to the opposing mica surface with W_{ad} = 2.5 ± 0.74 mJ/m^2 showing signatures of bridging *adhesion*.[1] The adhesion force between the protein film and the mica surface did not change significantly for C_{fp1} > 50 μg/ml. A similar bridging *adhesion* was measured for C_{fp1} = 100 μg/ml with W_{ad} = 2.61 ± 0.31 mJ/m^2 between the *mfp-1* (*Mc*) film and the mica surface. Protein films deposited at C_{fp1} = 25 μg/ml, however, did not show bridging *adhesion* against the mica surface and a sharp jump-out instability was measured during the separation of the surfaces (Fig S3a).

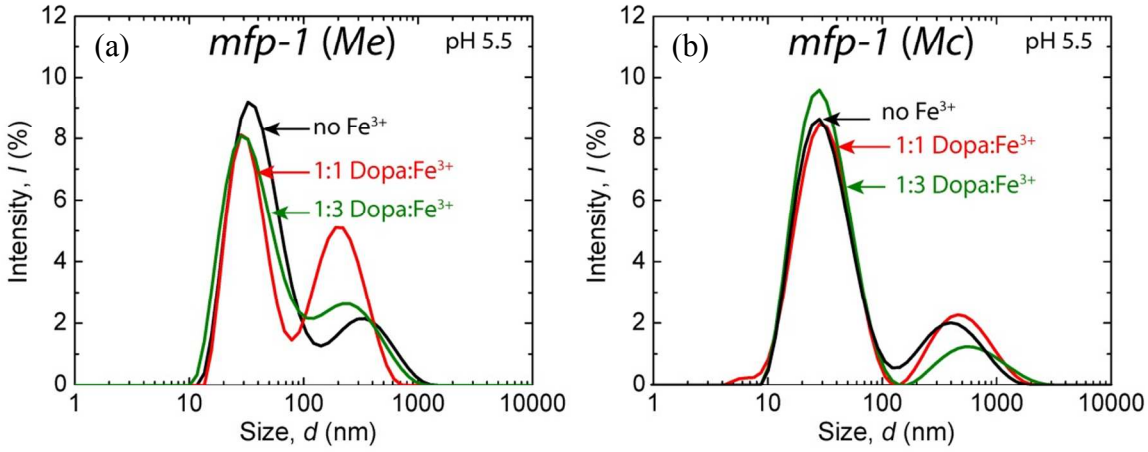

Figure S2. Effect of Fe^{3+} on aggregate size of *mfp-1* (*Me*) and *mfp-1*(*Mc*) by DLS measurements. In-solution aggregate size comparison of (a) *mfp-1*(*Me*) and (b) *mfp-1* (*Mc*) at 70 μg/ml were done in 0.1 M acetic acid, pH 5.5. Measurements were made with sequential increase in Fe^{3+} from 0 (no iron) to 1:1 and 3:1 (excess ratio) of iron to Dopa.

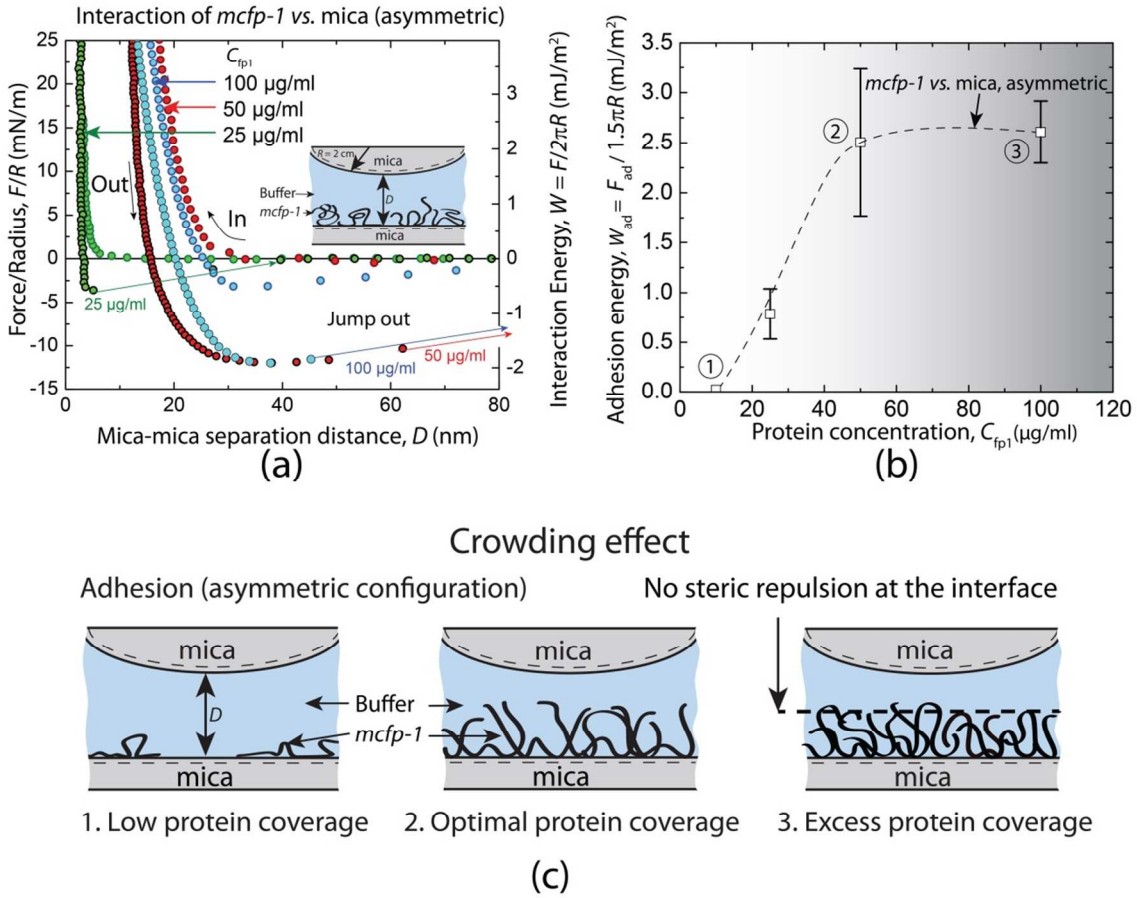

Figure S3. (a) Representative force *vs.* distance plot for different protein deposition concentrations (C_{fp1} = 25, 50 and 100 µg/ml in 0.1 M sodium acetate buffer, pH 5.5, 0.25 M KNO_3, and 1 mM bis-tris) showing adhesion between *mfp-1* (*Mc*) film and mica. (b) Effect of protein deposition concentration on the adhesion (*mfp-1*(*Mc*) *vs.* mcia, asymmetric) energies of interaction between the surfaces. (b) Schematic representations of the crowding effect for adhesion. The quality of the protein coverage (*viz*., low, optimal and excess) is based on the cohesion energy measred between protein films deposited at different bulk concentrations.

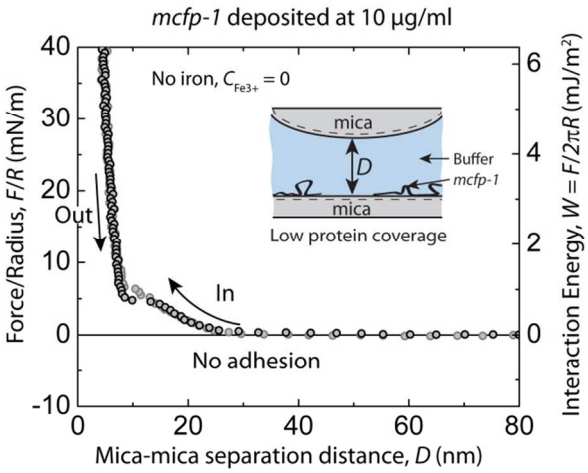

Figure S4. Representative force *vs.* distance plot showing the interaction between a bare mica surface and *mfp-1*(*Mc*) film deposited at 10 µg/ml in 0.1 M sodium acetate buffer, pH 5.5, 0.25 M KNO_3, and 1 mM bis-tris with C_{Fe3+} = 0 µM.

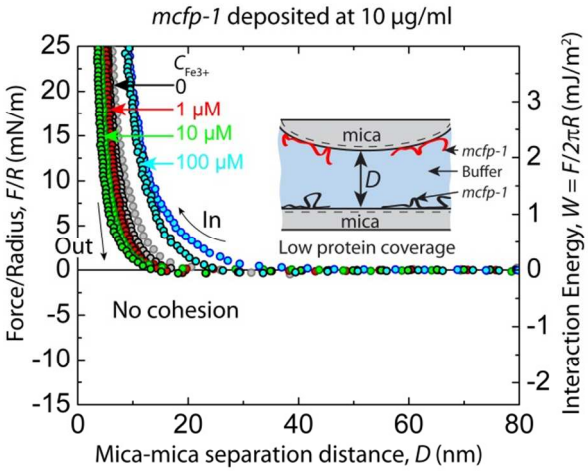

Figure S5. Representative force *vs.* distance plot showing the interaction between two symmetric *mfp-1* (*Mc*) films deposited at 10 µg/ml in 0.1 M sodium acetate buffer, pH 5.5, 0.25 M KNO_3, and 1 mM bis-tris with C_{Fe3+} = 0 µM (gray), C_{Fe3+} = 1 µM (red), 10 µM (green) and 100 µM (blue).

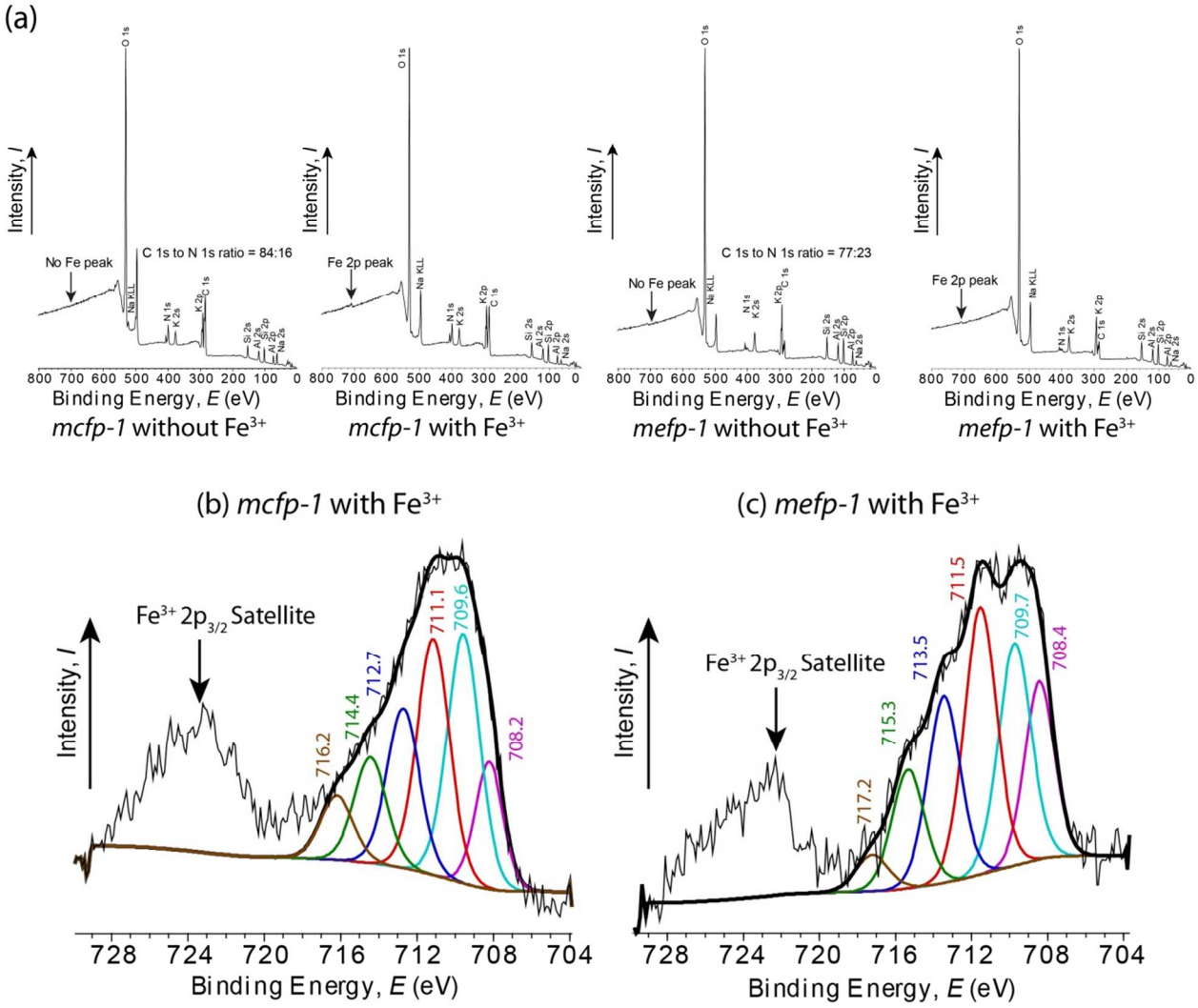

Figure S6. (a) XPS survey spectra on *mfp*-1(*Mc*) and *mfp*-1(*Me*) films deposited on mica surfaces at 50 µg/ml and 20 µg/ml respectively with and without preadsorbed Fe^{3+}. High resolution XPS Fe^{3+} 2p spectra on *mfp-1*(*Mc*) (b) and *mfp-1* (*Me*) (c) films with preadsorbed 50 µL of 10 µM Fe^{3+}, with Gaussian fits to the peaks.

X-ray photoelectron spectroscopy (XPS). The interaction of Fe^{3+} with the Dopa groups in *mfp-1* (*Mc*) and *mfp-1* (*Me*) were investigated by XPS (Axis Ultra XPS, Kratos Analytical, UK) spectrometer. A wide spectrum scan (Binding energy, E = 0 - 800 eV) was obtained with a pass energy of 160 eV (Fig. S6a). The binding energies were corrected to 285 eV for the C 1s peak.

High resolution elemental analysis of the N 1s and Fe 2p peaks were obtained at 40 eV pass energy with a step size of 0.1 eV and averaged over 2 scans (Fig. S6b). The experimental data was fitted to a Gaussian function.

Full spectrum scans of the *mfp-1*(*Mc*) and *mfp-1* (*Me*) films on mica surface are shown in Fig. S6a and no Fe peaks are detected in the protein films without pre adsorbed iron. High resolution XPS spectrum of the protein films with pre adsorbed Fe^{3+} shows that the coordination state of Fe^{3+} in the two adsorbed protein films is different [2]. The multiplets fitted to the Fe^{3+} $2p_{3/2}$ peak (Fig. S6b and c) shows higher energy peak fits to the Fe^{3+} coordinated to *mfp-1*(*Me*) compared to *mfp-1*(*Mc*) film. Decreased coordination will lower the electron density around ferric ion resulting in a higher energy needed to produce a photoelectron. Thus, the measurements made in the XPS demonstrate that *mfp-1*(*Me*) is better at wrapping Fe^{3+} compared to *mfp-1*(*Mc*).

Raman spectroscopy. Prior to testing with Raman spectroscopy, lyophilized protein samples were resuspended in 5 mM acetic acid to a concentration of 1 mg/ml. 1mM $FeCl_3$ was added to a droplet of the protein solution in a ratio of 3 DOPA residues to 1 Fe^{3+} ion and the pH was raised with NaOH. Raman micro spectroscopy was performed using a confocal Raman microscope (alpha300; WITec, Ulm, Germany) equipped with a piezoelectric scan stage (P-500, Physik Instrumente, Karlsruhe, Germany) and a Nikon objective (20X). A green laser (λ = 532 nm) was focused on the solution and Raman scattering was detected using a CCD camera (DV401-BV; Andor, Belfast, North Ireland) behind a spectrometer (UHTS 300; WITec) with a spectral resolution of 3 cm^{-1}. The Scan Ctrl Spectroscopy Plus software (version 1.38, Witec) was used for measurement setup and acquisition. Resonance Raman spectra were measured from several

different regions in the solution with an integration time of 0.5 s and 30 accumulations. For each sample, at least 4 spectra were averaged. Averaged spectra were baseline corrected and smoothed using OPUS software (Bruker, version 7.0).

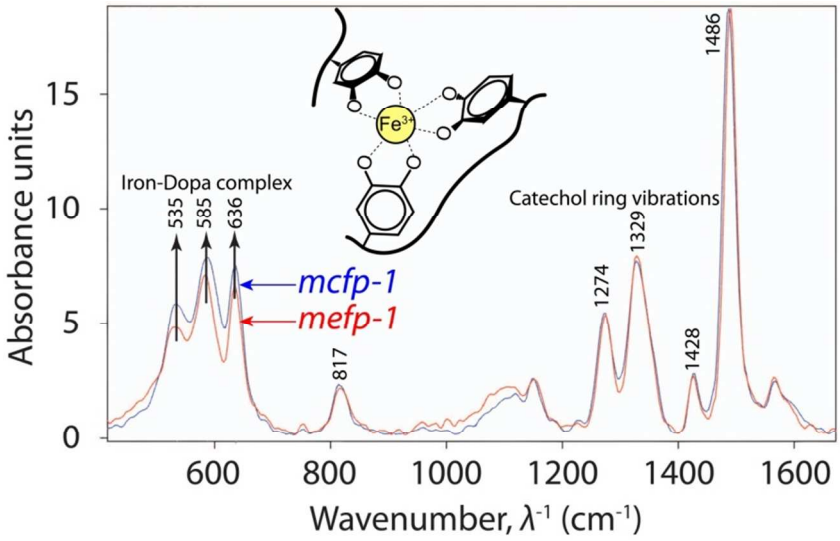

Figure S7. Resonance Raman microscopy of *mfp-1* (*Me*) and *mfp-1* (*Mc*) with Fe^{3+}. Prior to testing with Raman spectroscopy, samples were resuspended in 5 mM acetic acid to a concentration of 1 mg/ml. 1mM $FeCl_3$ was added to a droplet of the protein solution in a ratio of 3 Dopa residues to 1 Fe^{3+} ion. The pH was raised with NaOH (although it was possible to measure similar spectra even before adding the NaOH). Spectra were measured from different regions in the solution and at least 4 spectra were averaged. Data were background corrected and smoothed in OPUS.

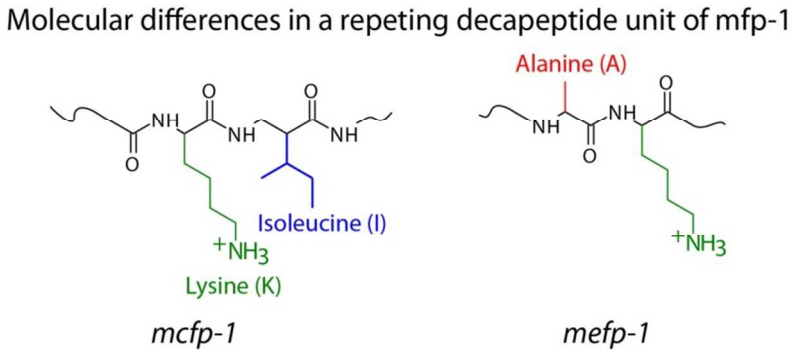

Figure S8. Molecular difference in the consensus decapeptide repeat unit of *mfp-1*(*Mc*) and *mfp-1*(*Me*).

Resolving the protein concentration values. The literature reports adhesion (asymmetric configuration) and cohesion (symmetric configuration) of *mfp-1* (*Mc*) protein films deposited at 10 μg/ml.[3, 4] However, it should be noted that the *mfp-1* (*Mc*) protein concentrations in the previous works were measured indirectly through Bradford protein assay. This work used a scalar method. Therefore, Bradford concentration assay standard curves were created with both bovine serum albumin (BSA) and *mfp-1* (*Mc*) to determine the dye binding capacity of *mfp-1* (*Mc*) compared to BSA, the standard protein used for making calibration curves for Bradford concentration assays. Comparing BSA binding to that of *mfp-1* (*Mc*) shows that *mfp-1* (*Mc*) has a 2.5 fold lower binding capacity than BSA, resulting in a 2.5 fold lower concentration reading than its BSA counterpart for the same protein concentration. Therefore, what previous studies indicate as 10 μg/ml, this study would indicate as 25 μg/ml (Fig. S9).

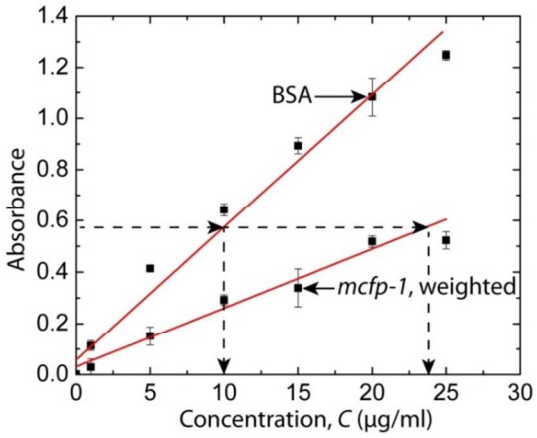

Figure S9: Bradford assay for *mfp-1* (*Mc*) and comparison to Bovine Serum Albumin (BSA).

Estimation of refractive index (n_P) of pure non-hydrated *mfp*-1(*Mc*)

Table S1. Molecular weight (M_A) and Refractive indices (n_A) of Amino Acids.

Amino acid	Molecular weight, M_A (g/mol)	Refractive Index, n_A
P*	131.1	1.540
K	146.2	1.615
I	131.2	1.568
S	105.1	1.676
Y*	197.2	1.654
P**	147.1	1.599
T	119.1	1.618

Mfp-1(*Mc*) from M. californianus has a mass of about 108 kDa and consists largely of tandem repeats of a decapeptide [P*KISY*P**P*TY*K], in which P*, P**, and Y* denote trans-4-hydroxyproline, trans-2,3,cis-3,4-dihydroxyproline, and 3,4-dihydroxyphenylalanine (Dopa), respectively.[5] The refractive index of the pure non-hydrated protein can be estimated from equation 1 as the weight average of the contribution from the individual amino acids refractive indices, n_A.[6]

$$n_P = \frac{\sum_A n_A M_A}{\sum_A M_A} \qquad [1]$$

Hence, for pure non-hydrated *mfp-1*(*Mc*), $n_P = 1.611$

Estimation of volume fraction of *mfp-1* (*Mc*) in the protein film from refractive index (n_F) measurements of the film

The refractive index, n_F, of the hydrated protein film was measured using Multiple Beam Interferometry (MBI) technique in the SFA experiments.[7] The volume fraction (V_P) of *mfp-1* (*Mc*) in the hydrated protein film confined between the mica surfaces under hard compression ($F/R > 30$ mN/m) was calculated using equation 2.

$$V_P = \frac{n_F - n_W}{n_P - n_W} \qquad [2]$$

where $n_W = 1.333$ (refractive index of water)

Table S2. Volume fraction (V_P) of *mfp-1*(*Mc*) in the hydrated protein film confined between the mica surfaces.

C_{mcfp-1} (µg/ml)	n_F	Volume fraction, V_P (%)
10	1.359	9
25	1.448	41
50	1.468	49
100	1.531	71

References

1. Das, S.; Donaldson Jr, S. H.; Kaufman, Y.; Israelachvili, J. N. *RSC Adv.* **2013,** *3*, 20405-20411.

2. Grosvenor, A. P.; Kobe, B. A.; Biesinger, M. C.; McIntyre, N. S. *Surf. Interface Anal.* **2004,** *36*, 1564-1574.

3. Zeng, H. B.; Hwang, D. S.; Israelachvili, J. N.; Waite, J. H. *Proc. Natl. Acad. Sci. U. S. A.* **2010,** *107*, 12850-12853.

4. Lu, Q. Y.; Hwang, D. S.; Liu, Y.; Zeng, H. B. *Biomaterials* **2012,** *33*, 1903-1911.

5. Holten-Andersen, N.; Zhao, H.; Waite, J. H. *Biochemistry* **2009,** *48*, 2752-2759.

6. Mcmeekin, T. L.; Groves, M. L.; Wilensky, M. *Biochem. Biophys. Res. Commun.* **1962,** *7*, 151-156.

7. Israelachvili, J.; Min, Y.; Akbulut, M.; Alig, A.; Carver, G.; Greene, W.; Kristiansen, K.; Meyer, E.; Pesika, N.; Rosenberg, K.; Zeng, H. *Rep. Prog. Phys.* **2010,** *73*.